

Microcalorimetric Determination of Thermodynamic Parameters for Ionophore–Siderophore Host–Guest Complex Formation

Stephen M. Trzaska, Eric J. Toone, and Alvin L. Crumbliss*

Department of Chemistry, Duke University, Box 90346, Durham, North Carolina 27708-0346

Received July 20, 1999

Thermodynamic parameters (ΔH , ΔS , and ΔG) were determined by microcalorimetry in wet chloroform for host–guest assembly formation involving second-sphere complexation of the siderophore ferrioxamine B by crown ether (18-crown-6, *cis*-dicyclohexano-18-crown-6, benzo-18-crown-6) and cryptand (2.2.2 cryptand) hosts. Similar data were also collected for the same hosts with the pentylammonium ion guest, which corresponds to the pendant pentylamine side chain of ferrioxamine B. Host–guest assembly formation constants (K_a) obtained from microcalorimetry agree with values obtained indirectly from chloroform/water extraction studies in those cases where comparable data are available. On the basis of a trend established by the pentylammonium guest, an enhanced stability relative to the crown ethers is observed for the assembly composed of ferrioxamine B and 2.2.2 cryptand that is due to entropic effects. Trends in ΔH and ΔS with changes in host and guest structure are discussed and attributed directly to host–guest complex formation, as solvation effects were determined to be insignificant ($\Delta C_p = 0$).

Introduction

Iron acquisition in microbes involves molecular recognition of an iron-siderophore complex at the cell membrane and subsequent transport through the membrane into the cell interior.^{1–4} Recognition takes place at a cell receptor site and two X-ray crystal structures have been reported recently for receptor-siderophore complexes.^{5,6} We are modeling molecular recognition via supramolecular host–guest assembly formation using low molecular weight host molecules. These hosts are used to mimic the high molecular weight membrane-bound protein receptors which effect cellular uptake of the siderophore.^{7–9} This approach provides a substitute for the protein receptors so that a variety of factors affecting assembly stability can be systematically monitored. What makes molecular

recognition possible is the fact that molecular guests bind more tightly to certain host molecules than others. Since this recognition increases the hydrophobicity of the guest complex these model studies also have application to phase transfer catalysis,¹⁰ metal extractions and precious/trace metal recovery,¹¹ and environmental remediation.^{12–14}

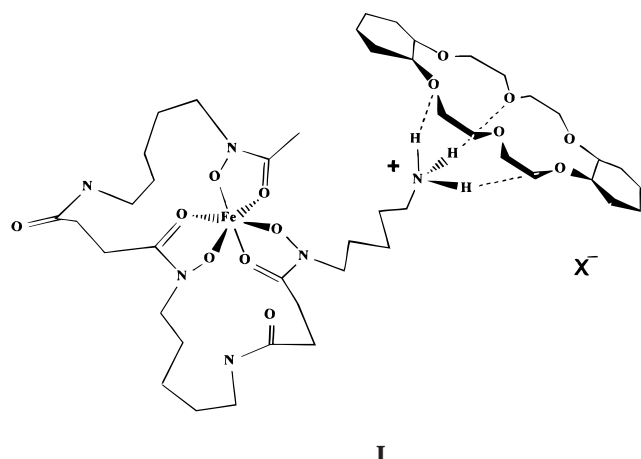
Our focus has been centered on the ferrioxamine B (FeH-DFB⁺)/crown ether supramolecular assembly **I**. This assembly is comprised of the protonated siderophore guest (RNH₃⁺), the ionophore host (H), and the counteranion (X[−]). Changes in any of these substituents have been shown to affect the host–guest association constant, K_a (eq 1).^{15–22} The magnitude of K_a in wet chloroform is sensitive to the second coordination shell of the guest and dependent on the degree of hydration of both the guest and the counteranion.^{15,16,20} Impor-

* Address correspondence to this author: E-mail: alc@chem.duke.edu. Fax: (919) 660-1605.

- (1) Crumbliss, A. L. In *Handbook of Microbial Iron Chelates*; Winkelmann, G. Ed.; CRC Press: Boca Raton, FL, 1991; p 177.
- (2) Raymond, K. N.; Telford, J. R. In *Bioinorganic Chemistry: An Inorganic Perspective of Life*; Kessissoglou, D. P., Ed.; NATO ASI Series C: Mathematical and Physical Sciences 459; Kluwer Academic Publishers: Dordrecht, The Netherlands; 1995; p 25.
- (3) Telford, J. R.; Raymond, K. N. In *Comprehensive Supramolecular Chemistry*; Lehn, J.-M., Executive Ed.; Pergamon Press: London, 1996; Vol. 1 (Molecular Recognition: Receptors for Cationic Guests) p 245.
- (4) Albrecht-Gary, A.-M.; Crumbliss, A. L. In *Iron Transport and Storage in Microorganisms, Plants, and Animals*; Sigel, A., Sigel, H. Eds.; Metal Ions in Biological Systems 35; M. Dekker, Inc.: New York, 1998; p 239.
- (5) Ferguson, A. D.; Hofmann, E.; Coulton, J. W.; Diedrichs, K.; Welte, W. *Science* **1998**, *282*, 2215.
- (6) Buchanan, S. K.; Smith, B. S.; Venkatramani, L.; Zia, D.; Lothar, E.; Palnitkar, M.; Chakraborty, R.; van der Helm, D.; Deisenhofer, J. *Nature Struct. Biol.* **1999**, *6*, 56.
- (7) Hiraoka, M., Ed. *Crown Ethers and Analogous Compounds*; Studies in Organic Chemistry, 45; Elsevier: Amsterdam, 1992.
- (8) Cox, B.; Schneider, H. *Coordination and Transport Properties of Macrocyclic Compounds in Solution*; Elsevier: Amsterdam, 1992.
- (9) Inoue, Y.; Gokel, G. W., Eds. *Cation Binding by Macromolecules*; Marcel Dekker Inc.; New York, 1990.

- (10) Dehmlow, E. V.; Dehmlow, S. S. *Phase Transfer Catalysis*; VCH: Weinheim; 1993.
- (11) Zolotov, Y. A., Ed. *Macrocyclic Compounds in Analytical Chemistry*; Chemical Analysis 143; Wiley-Interscience: New York; 1997.
- (12) Shukla, J. P.; Kumar, A.; Singh, R. K. *Sep. Sci. Technol.* **1992**, *27*, 447.
- (13) Raymond, K. N. In *Environmental Inorganic Chemistry*; Irgolic, K. J., Martell, A. E., Eds.; Proceedings of the U. S.-Italy International Workshop on Environmental Inorganic Chemistry, San Miniato, Italy, June 5–10, 1983; VCH: Deerfield Beach, FL, 1985; pp 331–347.
- (14) Lehn, J.-M.; Montavon, F. *Helv. Chim. Acta* **1978**, *61*, 67.
- (15) Spasojević, I.; Batinić-Haberle, I.; Choo, P. L.; Crumbliss, A. L. *J. Am. Chem. Soc.* **1994**, *116*, 5714.
- (16) Batinić-Haberle, I.; Crumbliss, A. L. *Inorg. Chem.* **1995**, *34*, 928.
- (17) Batinić-Haberle, I.; Spasojević, I.; Bartsch, R. A.; Crumbliss, A. L. *J. Chem. Soc., Dalton Trans.* **1995**, 2503.
- (18) Batinić-Haberle, I.; Spasojević, I.; Crumbliss, A. L. *Inorg. Chem.* **1996**, *35*, 2352.
- (19) Crumbliss, A. L.; Batinić-Haberle, I.; Spasojević, I. *Pure Appl. Chem.* **1996**, *68*, 1225.
- (20) Batinić-Haberle, I.; Spasojević, I.; Crumbliss, A. L. *Inorg. Chim. Acta* **1997**, *260*, 35.
- (21) Batinić-Haberle, I.; Spasojević, I.; Jang, Y.; Bartsch, R. A.; Crumbliss, A. L. *Inorg. Chem.* **1998**, *37*, 1438.
- (22) Caldwell, C. D.; Crumbliss, A. L. *Inorg. Chem.* **1998**, *37*, 1906.

tant factors involving the host include cavity size, dimensionality, flexibility, stereochemistry, and solvation shell.^{17–22} We have also demonstrated that second-sphere host–guest complexation



of ferrioxamine B can be used for selective bulk liquid membrane transport.^{23,24}

To better understand some of these factors influencing host–guest complex stability and bulk liquid membrane transport flux, thermodynamic parameters (ΔH , ΔS , and K_a) have been obtained by titration microcalorimetry and are reported here. The objectives of this study are to provide thermodynamic parameters for heretofore unreported host–guest systems in wet chloroform, to provide more information on certain crown ether and cryptand macrocycles, to independently confirm stability constants obtained in this laboratory through extraction experiments and bulk liquid membrane (BLM) studies, and to further explore the fundamental thermodynamic characteristics of the processes involved in siderophore-mediated iron acquisition through molecular recognition.

Experimental Section

Materials. Pentylamine (PA), *cis*-dicyclohexano-18-crown-6, a mixture of *syn* and *anti* isomers, benzo-18-crown-6, and 18-crown-6 were obtained from Aldrich and deferriferrioxamine B mesylate and 2.2.2 cryptand were obtained from Sigma and were used without further purification. Picric acid (HPic, Aldrich) was twice recrystallized from water. *Extreme care should be exercised when working with both picric acid and picrate salts.* Satisfactory purity levels were determined for all compounds by spectroscopic methods. Doubly deionized water and reagent grade chloroform were used in each experiment.

Aqueous Solutions. A magnesium picrate solution was prepared by neutralization of $Mg(OH)_2$ (Aldrich) with picric acid. Aqueous stock solutions containing the guest species ($FeHDFB^+, pic^-$) and (PA^+, pic^-) were prepared as described previously¹⁵ using magnesium picrate and the concentrations were determined spectrophotometrically to be 52 mM for ($FeHDFB^+, pic^-$) and 73 mM for (PA^+, pic^-).

Chloroform Solutions. Chloroform solutions of the crown ether and cryptand hosts were prepared at concentrations ca. 20 times greater than the respective guest solutions by dissolving appropriate amounts of material into a known volume of wet chloroform (prepared by water saturation). Chloroform solutions of ($FeHDFB^+, pic^-$) and (PA^+, pic^-) guests were prepared as follows. A 100 mL aqueous stock solution of either ($FeHDFB^+, pic^-$) or (PA^+, pic^-) was placed in a separatory funnel with 100 mL of $CHCl_3$. The funnel was shaken several times and the solution was allowed to come to equilibrium. The organic layer was collected and concentrated under reduced pressure. Several more chloroform extractions of the same aqueous solution and volume

reductions were performed until the desired concentration in wet $CHCl_3$ was achieved. The concentration was checked by adding a known volume of the chloroform solution (typically 1 mL) into a vial with a known amount of water (typically 10 mL). The vial was then shaken for 3 min and then centrifuged to separate the layers. For the ferrioxamine B solution, an aliquot of the top aqueous layer was passed through an anion-exchange resin (Dowex 1 \times 8–100, chloride form) to remove the light-absorbing picrate anion and the ferrioxamine B concentration was determined spectrophotometrically at 430 nm ($\epsilon = 2600 M^{-1} cm^{-1}$).²⁵ For the pentylammonium picrate solution, the picrate concentration was determined spectrophotometrically at 356 nm ($\epsilon = 14400 M^{-1} cm^{-1}$).²⁶ The concentrations of these guest solutions ranged from 0.39 to 14.6 mM, depending on the host species. UV–Vis spectra were acquired using a Hewlett-Packard 8451A diode array spectrophotometer.

Methods. Calorimetric measurements were performed using the Omega titration microcalorimeter from Microcal, Inc; details of the instrument design and data analysis are provided elsewhere.²⁷ Temperature control was maintained at 25.0, 35.0, or 45.0 (± 0.5) °C.

In a typical calorimetry experiment, 1.4 mL of a chloroform solution of guest ($FeHDFB^+, pic^-$ or PA^+, pic^-) was placed in the calorimeter. This solution was titrated with host in 40 injections of 2.5 μL each. The compensating power required to maintain thermal equilibrium between sample and reference cells is recorded as a function of time and integrated to yield a plot of enthalpy per injection as a function of ligand concentration. The heat evolved during each injection is a function of the enthalpy of binding ΔH and the amount of complex formed during that injection. This latter quantity is a function of the concentration of guest, host, complex and the host–guest association constant K_a . A nonlinear least-squares fit of the appropriate equation relating these values to the data provides estimates of ΔH , K_a , and the stoichiometry of binding n . A representative plot of ferrioxamine B picrate ($FeHDFB^+, pic^-$) interacting with 18C6 is shown in Figure 1; [$FeHDFB^+, pic^-$] = 5.92 mM and [18C6] = 130.2 mM. The top plot shows the heat evolved per unit time during each injection of host. The area under each peak is instrumentally computed, yielding the heat evolved per injection of host in $kcal mol^{-1}$ in the bottom plot.²⁷

Results and Discussion

Isothermal titration microcalorimetry offers a way of measuring ΔH and K_a for a host (H) interacting with a guest (RNH_3^+):



$$K_a = [H \cdot RNH_3^+, X^-] / [H][RNH_3^+, X^-] \quad (2)$$

$$-RT \ln K_a = \Delta H - T\Delta S \quad (3)$$

Calorimetric studies in water saturated chloroform were carried out for the association of two different guests interacting with various host species. The guests of interest are ferrioxamine B ($FeHDFB^+$; shown in **I**) and pentylammonium ion (PA^+), its pendant side chain without the Fe(III) complex. Picrate (pic^-) is the counterion. Comparative data for these two guests enable us to assess the influence of the siderophore second coordination shell on host–guest complexation. The hosts under investigation are 18-crown-6 (18C6, **II**), *cis*-dicyclohexano-18-crown-6 (DC18C6, **III**), benzo-18-crown-6 (B18C6, **IV**), and 2.2.2 cryptand (2.2.2, **V**). The results of these studies are shown in Table 1. Included in Table 1 are the $\log K_a$ values obtained indirectly through $CHCl_3/H_2O$ extraction experiments in this laboratory.¹⁸ Excellent agreement is observed between the two

(23) Spasojević, I.; Crumbliss, A. L. *J. Chem. Soc., Dalton Trans.* **1998**, 4021.

(24) Spasojević, I.; Crumbliss, A. L. *Inorg. Chem.* **1999**, 38, 3248.

(25) Monzyk, B.; Crumbliss, A. L. *J. Am. Chem. Soc.* **1982**, 104, 4921.

(26) Sadakane, A.; Iwachido, T.; Toei, K. *Bull. Chem. Soc. Jpn.* **1975**, 48, 60.

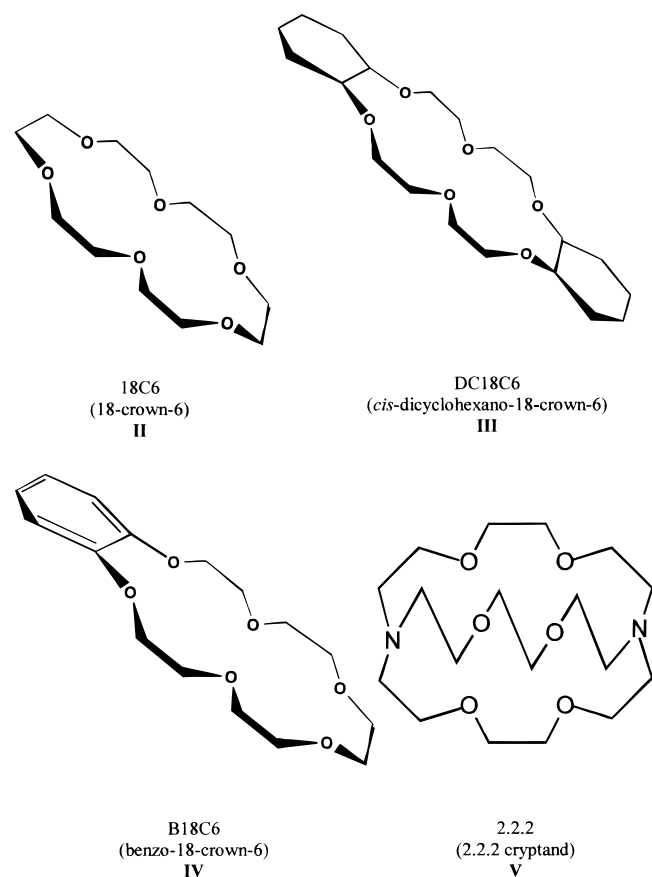
(27) Wiseman, T.; Williston, S.; Brandts, J. F.; Lin, L.-N. *Anal. Biochem.* **1989**, 179, 131.

Table 1. Thermodynamic Parameters for Host–Guest Complex Formation According to Eq 1^a

guest ^b	host ^c	log K_a^d	log K_a^e	ΔH^d (kJ mol ⁻¹)	$T\Delta S^{df}$ (kJ mol ⁻¹)	$T\Delta S^{ef}$ (kJ mol ⁻¹)
FeHDFB ⁺	18C6	3.52 (0.20)	3.80	-59.4 ^g (3.7)	-39.3	-37.7
PA ⁺	18C6	5.15 (0.07)		-60.5 (3.1)	-31.1	
FeHDFB ⁺	DC18C6	3.76 (0.07)	3.67	-37.4 (1.0)	-16.5	-17.0
PA ⁺	DC18C6	5.78 (0.22)	6.16	-36.6 (0.8)	-1.2	-0.4
FeHDFB ⁺	B18C6	2.82 (0.12)	2.81	-28.2 (1.3)	-12.1	-12.2
PA ⁺	B18C6	2.96 (0.11)		-28.9 (0.5)	-12.0	
FeHDFB ⁺	2.2.2	3.94 (0.09)	3.33	-50.2 ^h (3.5)	-27.7	-31.2
PA ⁺	2.2.2	4.35 (0.12)		-49.7 (1.1)	-24.9	

^a Data collected in wet CHCl₃ solution at 25 °C, using picrate salts of the guest. ^b FeHDFB⁺ = Ferrioxamine B; PA⁺ = pentylammonium. ^c 18C6 = 18-crown-6; DC18C6 = *cis*-dicyclohexano-18-crown-6; B18C6 = benzo-18-crown-6; 2.2.2 = 2.2.2 cryptand. ^d Determined from microcalorimetric titration at 25 °C. Values in parentheses represent experimental repeatability and are the std. deviations of the average of 3–5 independent determinations. Experimental uncertainties in data fits for individual runs were typically <3%. ^e Determined from CHCl₃/H₂O extractions at 25 °C.¹⁸ ^f $T = 25 \pm 0.5$ °C. ^g Value given for 25 °C. Values determined at 35 and 45 °C are -60.1 and -59.0 kJ mol⁻¹, respectively. ^h Value given for 25 °C. Values determined at 35 and 45 °C are -48.7 and -50.7 kJ mol⁻¹, respectively.

methods. A determination of K_a by a separate method also enables us to compute ΔS independently of ΔH , which eliminates any coupled errors in $\Delta H/\Delta S$ pairs.



There are a few salient features exhibited by the data in Table 1. The magnitude of the host–guest association constant K_a for each system denotes a stable supramolecular assembly. All of the ΔH values are negative, indicating exothermic binding, as expected for stable host–guest complexes based on H-bonding interactions between a protonated amine and ether oxygen atoms. The entropic terms are all negative, consistent with an increase in order upon complexation. Specifically, these are enthalpy stabilized complexes, in which $\Delta H < 0$ and dominant, and $T\Delta S < 0$.

While it is tempting to interpret changes in thermodynamic parameters for a host–guest association in terms of differences in solute–solute interactions, the role of solvation cannot be

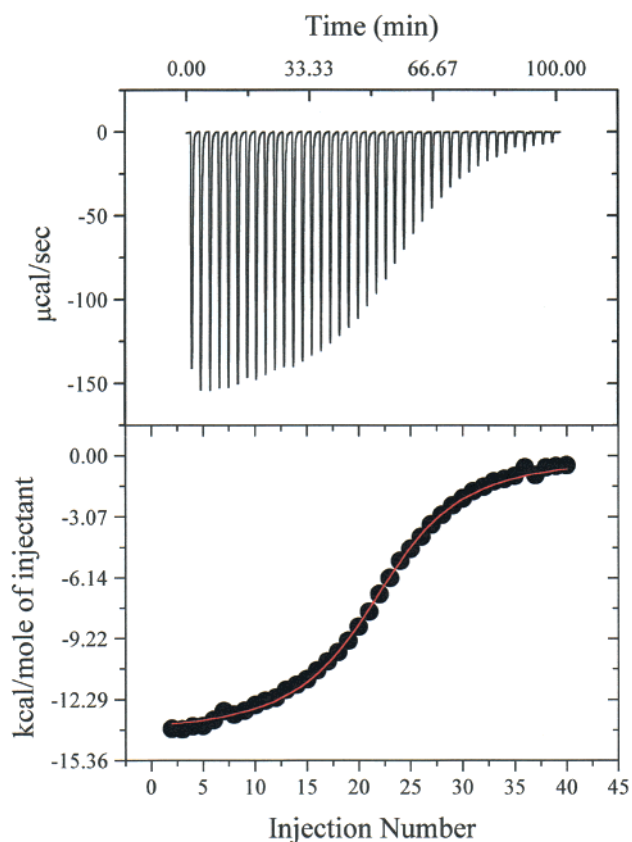


Figure 1. Sample data for the microcalorimetry titration of a 5.92 mM (FeHDFB⁺,pic⁻) solution by a 130.2 mM solution of the crown ether 18C6. The titration was carried out with 40 2.5 μ L injections of 4.4 s duration with 2.5 min intervals between injections. The top plot shows the heat evolved per time during each injection of host. The area under each peak is calculated, yielding the heat evolved per injection in kcal/mol of host in the bottom plot. Fitting the integrated data yields a host–guest binding constant (K_a) for {18C6·FeHDFB⁺,pic⁻} of 4878 ± 196 M⁻¹ (log $K_a = 3.69 \pm 0.02$) and an enthalpy of binding (ΔH) of -14109 cal mol⁻¹ (-59.0 kJ mol⁻¹) at 25.0 °C.

discounted. Indeed, in association processes in aqueous solution differences in interactions of the various species—guest, host, and complex—with water are typically greater than differences in interactions between the solutes. On the other hand, solvation effects are much less important during association events in organic solvents. The role of water cannot, a priori, be discounted here because of the water saturated chloroform solvent system used. Accordingly, we sought to rigorously evaluate the contribution of solvation effects during host–guest binding. One of us has previously demonstrated that the change

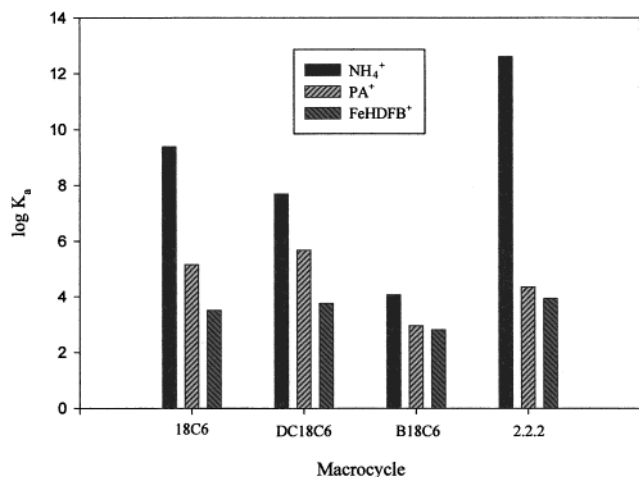


Figure 2. Histogram showing variation of host-guest binding constant with host structure for ferrioxamine B (FeHDFB⁺), pentylammonium (PA⁺), and NH₄⁺ guests. {2.2.2·NH₄⁺,pic⁻} data obtained from NMR studies in D₂O saturated CDCl₃,³¹ {B18C6·NH₄⁺,SCN⁻} data obtained calorimetrically in MeCN,³² {DC18C6·NH₄⁺,pic⁻}¹⁵ and {18C6·NH₄⁺,pic⁻}³³ data obtained from CHCl₃/H₂O extractions at 25 °C.

in molar heat capacity (ΔC_p), or the temperature dependence of the enthalpy of binding, is exclusively a measure of the contribution of solvation to binding thermodynamics.²⁸ The change in ΔC_p during the binding of FeHDFB⁺ to both 18C6 and 2.2.2 cryptand is zero (see Table 1, footnotes *g* and *h*), suggesting that changes in solvation do not contribute significantly to the thermodynamic parameters for the host-guest complexation reactions reported here. We thus interpret changes in host-guest binding thermodynamics to changes in solute-solute interactions.

The enthalpy of binding appears to be a function of the host. The essentially equivalent enthalpy values for FeHDFB⁺ and PA⁺ complexing with the same crown ether host (18C6, DC18C6, or B18C6) and 2.2.2 cryptand is consistent with the same intermolecular interactions; i.e. host-guest complex formation via three hydrogen bonds to the ether oxygen atoms. Therefore, changes in K_a for different guests with each macrocyclic host are due to entropic differences.

The magnitude of the ΔH values for both guests with the hosts increases in the order: 18C6 (-60) > 2.2.2 (-50) > DC18C6 (-37) > B18C6 (-28 kJ mol⁻¹). The decrease in exothermicity relative to 18C6 for the two substituted 18C6 macrocycles can be readily explained. Adding two cyclohexano substituents to the 18C6 cavity provides steric bulk and hinders the ability of this DC18C6 host to adjust to the substituted ammonium guest. Furthermore, attaching a benzo substituent to the 18C6 cavity decreases ring flexibility and decreases the basicity of the oxygen atoms of the B18C6 host, thus abating H-bonding between the host and guest. This electronic effect causes an even greater increase in ΔH than is seen with DC18C6.

In general, the cryptate effect is defined as the enhanced stability of a macrobicyclic complex compared to a macro-monocyclic complex. This effect is mostly enthalpic in origin and also results from a lower degree of solvation in the macrobicyclic compound.^{29,30} Figure 2 demonstrates the variation in $\log K_a$ with host structure for FeHDFB⁺, PA⁺, and NH₄⁺ guests. NMR equilibration studies carried out in wet chloroform

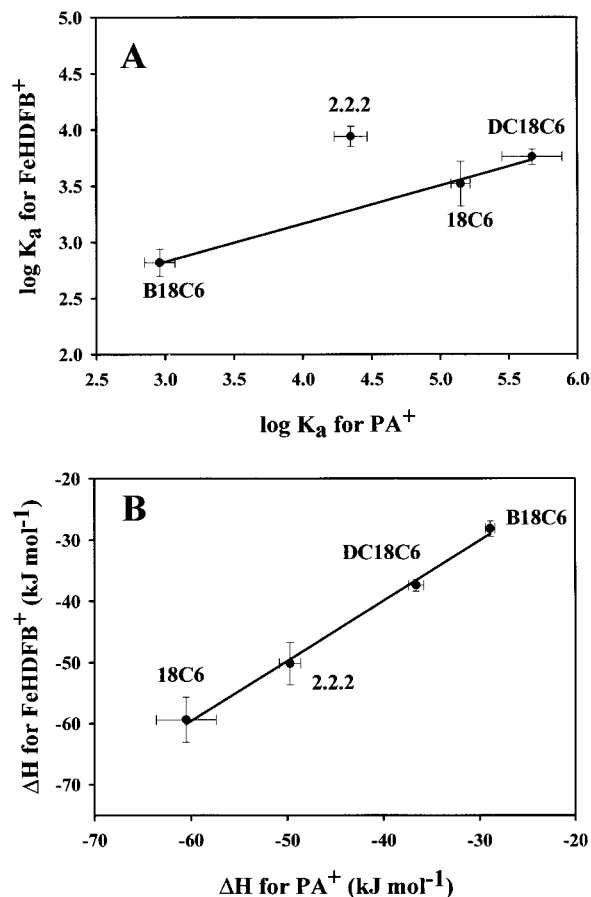


Figure 3. (A) Plot of stability constants ($\log K_a$) of FeHDFB⁺ assemblies vs PA⁺ assemblies. Regression line ($R^2 = 0.996$, slope = 0.339, intercept = 1.81) defined only for crown ether data. (B) Plot of enthalpies for host-guest assemblies of FeHDFB⁺ vs those of PA⁺. Crown ether and cryptand data define regression line ($R^2 = 0.996$, slope = 0.982, intercept = -0.67 kJ mol⁻¹).

revealed a high association constant for 2.2.2 cryptand and ammonium picrate with a $\log K_a$ of 12.6.³¹ We would expect the host-guest association constants for FeHDFB⁺ and PA⁺ to be less than that of NH₄⁺. While NH₄⁺ fits nicely within the cryptand cavity,³⁴ FeHDFB⁺ and PA⁺ have side chains that prevent total encapsulation. This causes a decrease in K_a by more than 8 orders of magnitude. Apparently the cryptate effect is most effective for those cations which can fit within the cryptand cavity. Otherwise, there is little, if any, increase in K_a . Figure 2 illustrates the classical cryptand effect for NH₄⁺ by demonstrating a significantly higher affinity for 2.2.2 cryptand over 18C6. This enhancement is not observed for FeHDFB⁺, suggesting the classical cryptate effect is not seen for this guest due to its steric bulk which prevents the protonated amine chain (RNH₃⁺) from residing in the 2.2.2 cryptand cavity. For the supramolecular assemblies described here, the cryptand can essentially be considered as a two-dimensional diaza-18-crown-6 with a cyclic backbone. While the backbone has a considerable amount of flexibility, the change from 6

(28) Chervenak, M. C.; Toone, E. J. *J. Am. Chem. Soc.* **1994**, *116*, 10533.

(29) Marsicano, F.; Hancock, R. D.; and McGowan, A. *J. Coord. Chem.* **1992**, *25*, 85.

(30) Hancock, R. D.; Martell, A. E. *Comments Inorg. Chem.* **1988**, *6*, 237.

(31) Cram, D. J.; Ho, S. P. *J. Am. Chem. Soc.* **1986**, *108*, 2998.

(32) Solov'ev, V. P.; Strakhova, N. N.; Raevskii, O. A. *Abstracts of Papers*; 13th International Symposium on Macrocyclic Chemistry, Hamburg, Sept 4-8, 1988.

(33) (a) Izatt, R. M.; Pawlak, K.; Bradshaw, J. S.; Bruening, R. L. *Chem. Rev.* **1991**, *91*, 1721. (b) Izatt, R. M.; Bradshaw, J. S.; Nielsen, S. A.; Lamb, J. D.; Christensen, J. J. *Chem. Rev.* **1985**, *85*, 271.

(34) Lehn, J.-M. *Supramolecular Chemistry: Concepts and Perspectives*; VCH: New York, 1995; p 24.

oxygen to 4 oxygens and 2 nitrogens leads to a less exothermic enthalpy change than with 18C6 (Table 1).

Figure 3A demonstrates relative trends in K_a for FeHDFB^+ and PA^+ by showing a plot of $\log K_a$ for FeHDFB^+ vs $\log K_a$ for PA^+ . The crown ether data define a reasonable linear relationship. These data illustrate that PA^+ forms more stable complexes than FeHDFB^+ , which is attributed to the steric bulk of the siderophore attached to the pendant amine sidearm. A slope of ca. 0.3 for the linear relationship intimates that FeHDFB^+ is less sensitive than PA^+ to host structural changes, since the less sterically hindered PA^+ can more closely approach the host. Data for 2.2.2 cryptand lies above the line, which demonstrates that $\log K_a$ is either lower than expected for PA^+ , or higher than expected for FeHDFB^+ . There may, of course, be other reasons why 2.2.2 cryptand does not follow the trend established by the other macrocycles, which may include cryptand interaction with the primary chains connecting the hydroxamate units in the siderophore.

Figure 3B describes relative trends in ΔH for FeHDFB^+ and PA^+ guests. This plot helps to explain the behavior of 2.2.2 cryptand illustrated in Figure 3A. Here, the crown ethers and 2.2.2 cryptand form a well-defined line. This demonstrates that the enhanced stability of the FeHDFB^+ assembly with 2.2.2 cryptand is entropic in origin.

Figure 4 is a plot of ΔH vs ΔS for all assemblies investigated and illustrates a general trend whereby changes in ΔH are compensated by changes in ΔS . Where possible, ΔS values were calculated using K_a from independent extraction studies¹⁸ (see Table 1, columns 4 and 7), which means the x and y axes in Figure 4 represent independent measurements and errors in ΔH and ΔS values are not coupled. Although there is appreciable scatter, the plot still clearly denotes a correlation.³⁵ Assemblies exhibiting gains in enthalpic stability (i.e., more negative ΔH) are met with unfavorable entropy changes. Since we have ruled out the influence of solvation effects on our thermodynamic parameters, this trend may be interpreted in the context of an isolated host and guest coming together to form a stable host–guest assembly. A more tightly bound assembly held together

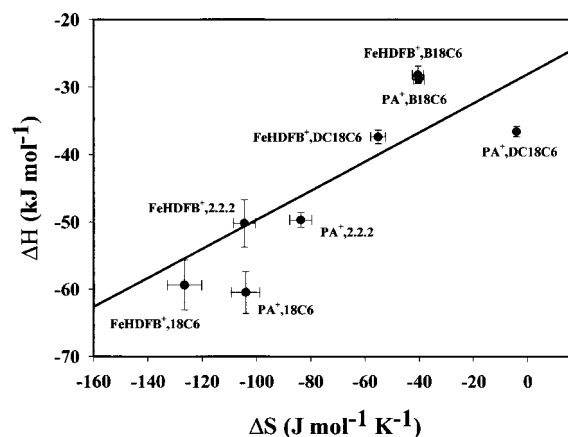


Figure 4. Plot of ΔH vs ΔS for eq 1 in wet chloroform at 25 °C. ΔH data taken from microcalorimetry experiments as listed in Table 1. ΔS data calculated from K_a (eq 1) values¹⁸ obtained from independent water/chloroform extraction experiments (Table 1) for {DC18C6·PA⁺,pic⁻} and all FeHDFB^+ assemblies; these data points define the regression line ($R^2 = 0.85$) where $T_{\text{iso}} = 216$ K was calculated from the slope.³⁵

through H-bonding will produce a more exothermic reaction and result in a greater loss of entropy. That is, it is anticipated that a simple host–guest assembly formation from isolated host and guest moieties, such as illustrated in eq 1, with minimal solvation effects, will produce a compensation plot such as shown in Figure 4.³⁸ The slope³⁵ of the plot in Figure 4 suggests an isothermal temperature below 298 K, which is consistent with changes in K_a at 298 K with changing host and guest structure being controlled by fluctuations in entropy.

Acknowledgment. We are grateful for the financial support of the NSF and the Petroleum Research Fund of the American Chemical Society.

IC9908571

(35) The data plotted in Figure 4 pass the test of Petersen, et al.³⁶ and Wiberg³⁷ for statistical significance for a valid linear correlation. However, this does not preclude the existence of more than one isothermal relationship.

(36) Petersen, R. C.; Markgraf, J. H.; Ross, S. D. *J Am. Chem. Soc.* **1961**, *83*, 3819.

(37) Wiberg, K. B. *Physical Organic Chemistry*; Wiley: New York, 1964; pp 376–379.

(38) Gokel, G. *Crown Ethers & Cryptands*, The Royal Society of Chemistry; London; 1994; pp 76–78.